

The Effect of a High Thermal Gradient on Sintering and Stiffening in the Top Coat of a Thermal Barrier Coating (TBC) System

S.A. Tsipas, I.O. Golosnoy and T.W. Clyne

*Department of Materials Science and Metallurgy, University of Cambridge
Pembroke Street, Cambridge CB2 3QZ, UK*

Abstract

Superalloy substrates coated with plasma sprayed CoNiCrAlY bond coats and yttria-stabilized zirconia top coats have been subjected to a high heat flux in a controlled atmosphere chamber. The sintering exhibited by the top coat under these conditions has been studied and compared with the behavior observed during isothermal heating, both when attached to the substrate and when detached. Sintering has been characterized by (a) microstructural examinations, (b) dilatometry, in both in-plane and through-thickness directions, and (c) stiffness measurements, using both cantilever bending and nanoindentation. A numerical heat flow model has been used to explore the stress state under isothermal and thermal gradient conditions. Sintering proceeds faster at higher temperature, but is retarded by the presence of tensile stresses (from differential thermal expansion between coating and substrate) within the top coat. Sintering occurs preferentially near the free surface of the top coat under gradient conditions, not only because of the higher temperature, but also because the in-plane stress is more compressive in that region.

Introduction

Failure of TBCs commonly occurs by buckling and spalling of the top coat [1-7]. The strain tolerance of the top coat is important and this has been extensively studied for both EB-PVD and plasma sprayed systems. For plasma sprayed top coats, this strain tolerance is enhanced by a high compliance, which is largely a consequence of the presence of many fine microcracks and pores in the microstructure. This low stiffness inhibits the build-up of large stresses, and hence large driving forces for spallation. Recent work [8] has confirmed that, while APS and VPS top coats have low in-plane Young's moduli in the as-sprayed state, healing of microcracks due to sintering raises the stiffness substantially during holding at temperatures similar to those experienced in service. This stiffening will raise the strain energy release rate associated

with a given misfit strain and hence make spallation more likely.

It is also important to recognize that service conditions involve the presence of a high through-thickness thermal gradient, which will modify the residual stress distribution. This will affect the driving force for spallation and might also be expected to influence the sintering characteristics. The current paper is aimed at investigating the thermo-mechanical stability and spallation of TBCs, with particular reference to the effect of a high thermal gradient.

Experimental Procedures

Coating Production. The powders were supplied by Sulzer-Metco (US) Inc. The bond coat material, designated Amdry 995C, has a nominal composition (in wt%) of Co-32Ni-21Cr-8Al-0.5Y. The top coat was yttria-partially-stabilized-zirconia (ZrO_2 -7wt% Y_2O_3), designated 204NS-1. The powders were deposited onto Nimonic 80A substrates 50 mm thick and mild steel substrates 1.5 mm thick. Specimens were produced by vacuum plasma spraying (VPS) of the bond coat, followed by air plasma spraying (APS) of the top coat, using the conditions shown in Table 1. The bond coats were about 140 μm in thickness and the top coats varied between about 1.5 and 2.6 mm.

Table 1: Plasma Spraying Parameters.

Spraying Parameters	Deposit Material	
	CoNiCrAlY	ZrO_2 - Y_2O_3
Type of Spraying	VPS	APS
Spraying distance (mm)	270	105
Arc Current (A)	500	750
Voltage (V)	50	60
Gun speed (mm s^{-1})	100	55
Nozzle diameter (mm)	8	8
Ar flow Rate (l min^{-1})	50	50
H_2 flow rate (l min^{-1})	10	8
Chamber pressure (mbar)	200 (Ar)	1000 (air)

Heat Treatment. A specially designed heat treatment rig was employed, in which a high thermal gradient could be maintained. A schematic of the set-up, and a photo of the rig, are shown in Fig.1. The base of the substrate was brazed to a water-cooled copper block. Insulation was placed around the specimen to minimize lateral heat losses. The graphite susceptor could be lifted away from the induction coil by a hydraulic ram, allowing thermal cycling of the specimen. The holding time at temperature, for each thermal cycle, was 1 h and samples were allowed to cool to room temperature before being re-heated. Heating rates were $\sim 20 \text{ K min}^{-1}$ and cooling rates $\sim 30 \text{ K min}^{-1}$. The thermal gradient was monitored and controlled by four thermocouples embedded in the substrate. The chamber incorporated a viewing window. The temperature at the free surface of the top coat was monitored using an optical pyrometer. Isothermal heat treatments of detached samples were also performed in the same chamber, at temperatures in the range 1200-1400°C. A vacuum of 2×10^{-4} mbar was maintained throughout.

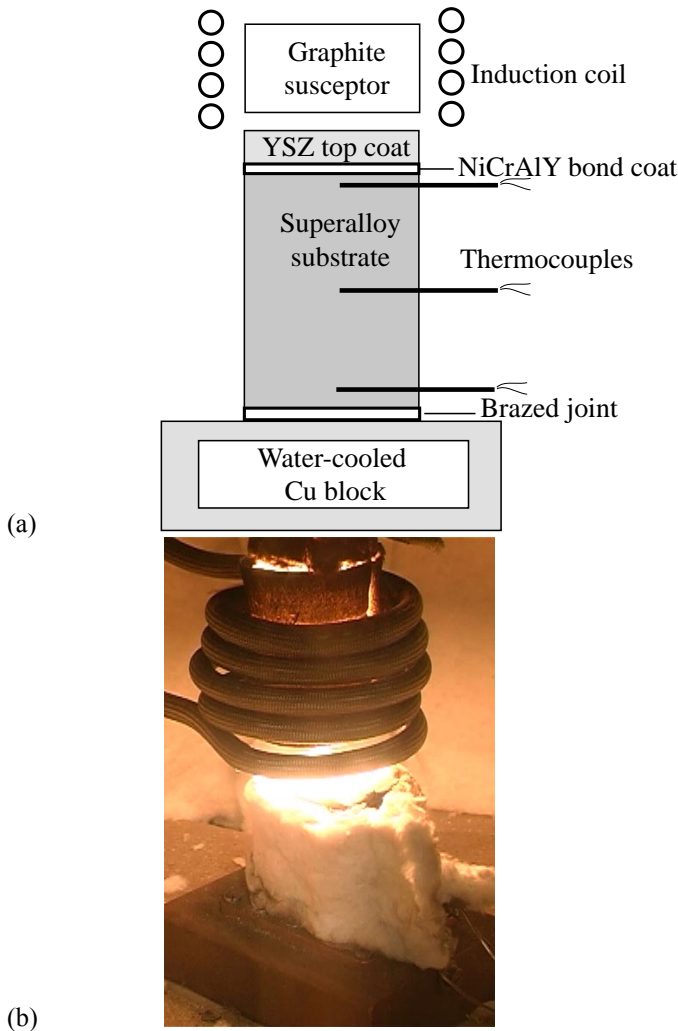


Figure 1: The high thermal gradient rig: (a) schematic diagram and (b) photo taken during operation.

A TBC with a 2.65 mm thick top coat was thermally cycled, such that the specimen spent a total of 47 h at the maximum temperature. The thermal profile at steady state is shown in Fig.2. Experimental data are shown from the thermocouples and the pyrometer, together with predictions from a numerical heat flow model [9, 10]. It can be seen that the thermal profile is consistent with a top coat conductivity of about $1.0 \text{ W m}^{-1} \text{ K}^{-1}$.

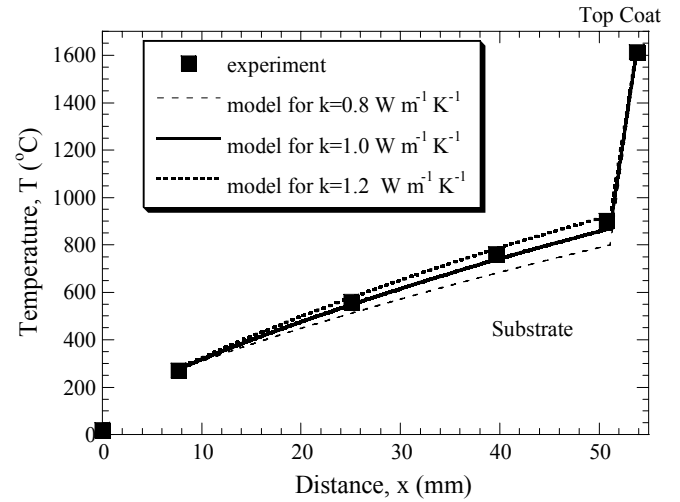


Figure 2: Thermal profile through the thickness of the TBC system at steady state. The modeled profiles correspond to three different values for the thermal conductivity of the top coat.

Dimensional, Stiffness and Microstructural Changes. Length changes during heat treatment were measured with a Netzsch DIL 402C dilatometer. Dilatometry was performed on detached top coats, in both in-plane and through-thickness directions. Top coats were detached from steel substrates using hydrochloric acid. Top coat fracture surfaces were examined using a JEOL 5800LV scanning electron microscope. Stiffness measurements were made using both cantilever bending and nanoindentation. Details of the cantilever bend testing are given elsewhere [8]. Nanoindentations were made on polished transverse sections, using a MicroMaterials NanoTest 600 indenter. Regions remote from obvious microcracks and pores were chosen for performing indentations. The maximum load was 100 mN and the loading rate was 5.1 mN s^{-1} . X-ray diffraction for phase identification was carried out using a computer-controlled Phillips PW1710 diffractometer, to study top coat phase constitutions.

Dilatometry

Dilatometry data are presented in Fig.3. The linear contraction is plotted against time at temperature. Contraction (shrinkage) occurs due to sintering of the coatings. For a given direction, the sintering is faster at higher temperature,

and in all cases the rate of contraction falls off with time. These results are broadly consistent with previous studies of sintering in top coats [11-14] and of rates of stiffness change [8, 15]. It is also clear that more contraction occurs in the through-thickness direction than in the in-plane direction. This effect does not appear to have been reported previously. The pore shape and distribution in plasma sprayed coatings, which are such that the inter-pore spacings are lower in the through-thickness direction, are probably responsible for this effect. A model for the sintering process is currently being developed, in which matter redistribution is such that contraction is expected to be greater in the through-thickness direction.

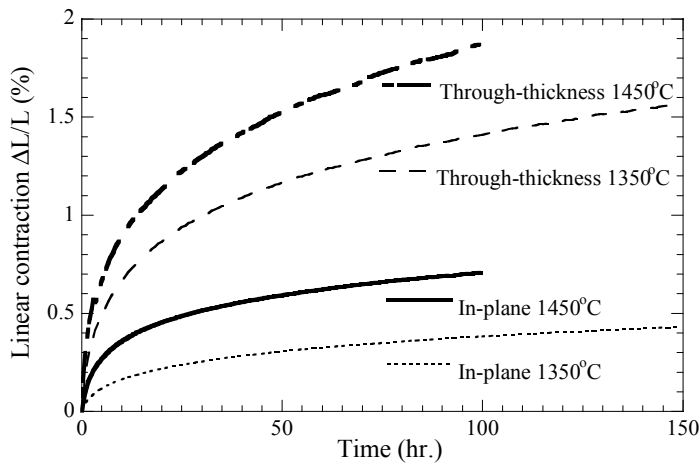


Figure 3: Dilatometry plots obtained during heat treatment of detached top coats.

Microstructural Examination

Isothermal heat treatment. Figure 4 shows SEM micrographs of fracture surfaces of YPSZ. As-sprayed coatings exhibit the characteristic splat structure of PS coatings. The grain structure within individual splats is columnar. Microcracks and pores are also present. Heat treatment results in grain growth between splats in close physical proximity. There is also evidence of the healing of microcracks.

Heat Treatment Under a High Thermal Gradient. Figure 5 shows SEM micrographs of the top coat after heat treatment with a thermal gradient. It can be seen that, near the TC/BC interface, there has been relatively little sintering. Microcracks are still present and bonding between splats is poor. Grains in individual splats have maintained their columnar structure. Near the free surface of the TC, on the other hand, pronounced sintering has taken place. There has been extensive healing of microcracks and grain growth has occurred, with many grains becoming both larger and more equiaxed in morphology.

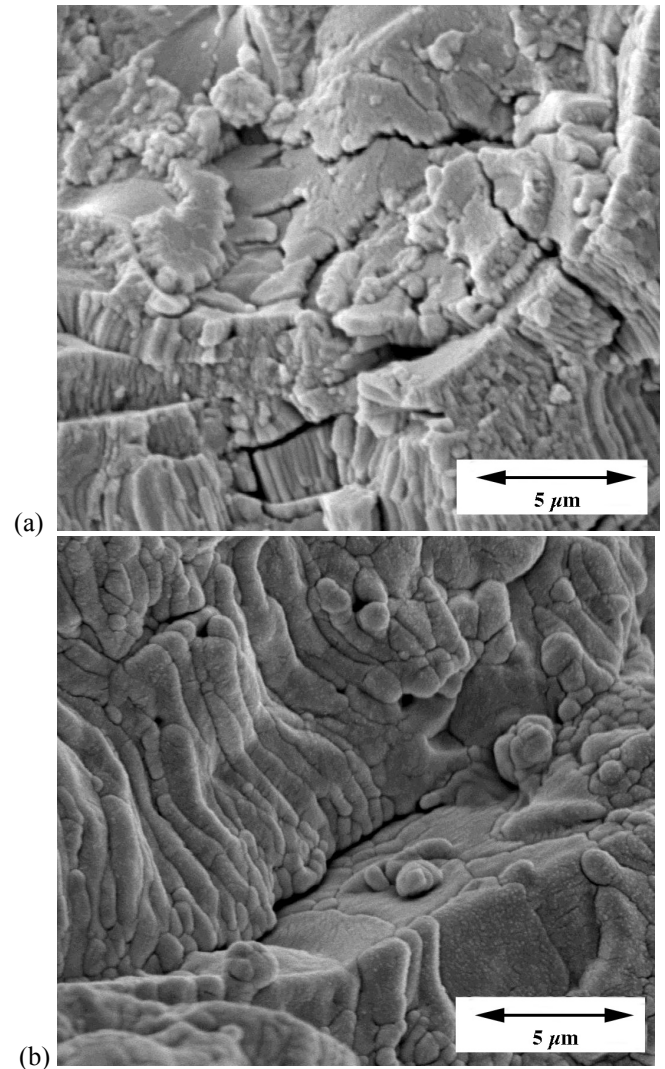


Figure 4: SEM micrographs of fracture surface of $\text{ZrO}_2\text{-Y}_2\text{O}_3$ top coats (a) as-sprayed and (b) after isothermal heat treatment at 1300°C for 100 hours.

Phase Constitution

XRD spectra obtained from top coats are presented in Figs. 6 and 7, covering 2θ ranges in which characteristic peaks appear when the tetragonal, monoclinic and cubic phases exhibited by YSZ are present. Figure 6 shows that essentially only the non-transformable tetragonal T' phase is present throughout the as-sprayed top coat and also in the thermal gradient treated material, close to the interface with the bond coat. Just a trace of the monoclinic phase is evident in these scans. In Fig. 7, on the other hand, it can be seen that relatively high levels of the cubic (F) phase (~35% from peak area analysis) are present in the isothermally heat treated material. In the thermal gradient treated material located near the free surface, on the other hand, the XRD spectra indicate a mixture of low- and high-

yttria tetragonal phases (T'1 and T'2), which were formed on cooling from the high temperature tetragonal (T) and cubic (F) phases respectively. These results are broadly consistent with features of the $\text{ZrO}_2\text{-Y}_2\text{O}_3$ phase diagram [16].

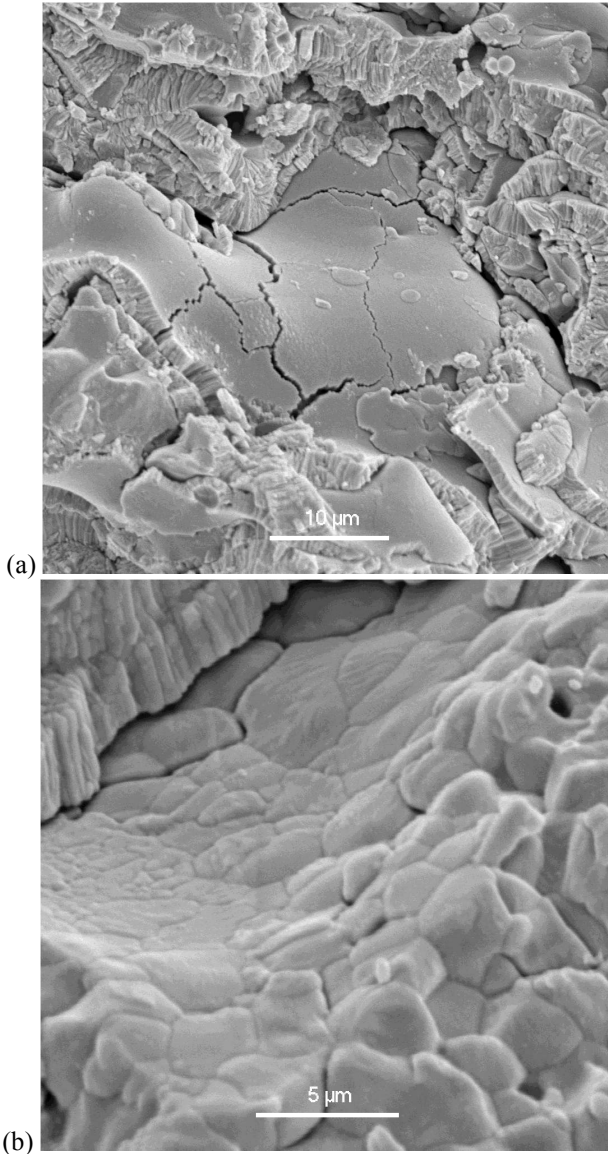


Figure 5: SEM micrographs of a $\text{ZrO}_2\text{-Y}_2\text{O}_3$ top coat after exposure to a high thermal gradient for 17 h, (a) near the TC/BC interface and (b) near the TC outer surface.

Stiffness Measurements

Cantilever bending. This technique, which measures the global in-plane stiffness of the coating, was applied to as-sprayed top coats. The value obtained was 10 ± 2 GPa. This was found to increase to around 60 ± 10 GPa after a heat treatment of about 100 h at 1300°C .

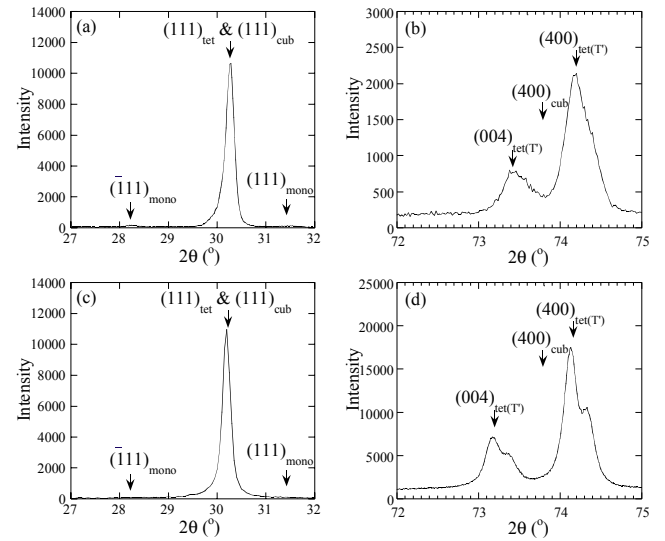


Figure 6: XRD spectra in the 2θ range $27\text{-}32^\circ$ and $72\text{-}75^\circ$ for $\text{ZrO}_2\text{-Y}_2\text{O}_3$ top coats, (a) & (b) as-sprayed and (c) & (d) after gradient heat treatment (Fig.2), near the interface with the bond coat.

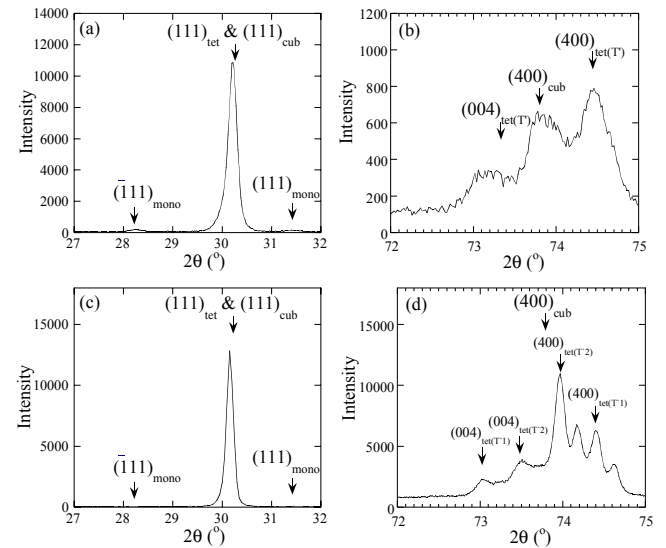


Figure 7: XRD spectra in the 2θ range $27\text{-}32^\circ$ and $72\text{-}75^\circ$ for $\text{ZrO}_2\text{-Y}_2\text{O}_3$ top coats, (a) & (b) after isothermal heat treatment for 100 h at 1300°C and (c) & (d) after gradient heat treatment (Fig.2), near the free surface.

Nanoindentation. Measurements were made on a top coat that had been heat treated for 17 h under high heat flux conditions. Data are shown in Fig.8. A through-thickness gradient in the stiffness is apparent. Near the TC/BC interface, values were similar to those obtained with the as-sprayed top coat, but near the outer surface the average value increases, approaching that of monolithic dense YSZ. There is, of course, quite a lot of scatter in the data, since the value obtained will be sensitive to the presence or absence of neighboring fine scale flaws. These results are consistent with the microstructural

observations, indicating pronounced sintering near the outer surface. The absolute values of Young's modulus obtained using this technique are, as expected, much higher than those given by methods that measure the global stiffness, since gross flaws affect the latter, but not the former.

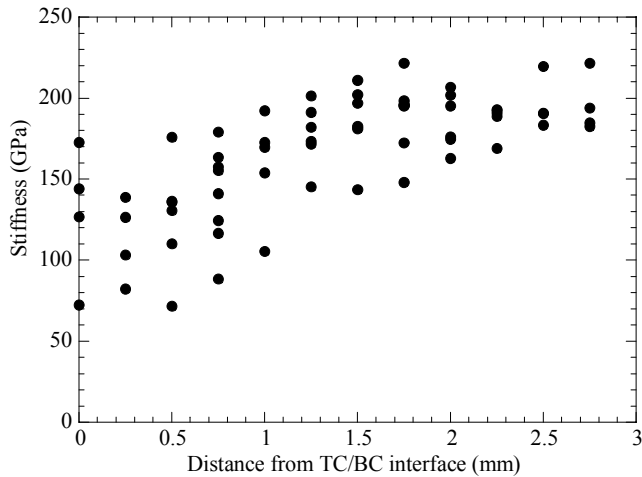


Figure 8: Stiffness data obtained by nanoindentation on a polished transverse section of a top coat after heat treatment in thermal gradient for 17 h.

Stress State during Heat Treatment

A model developed by Clyne and co-workers [10, 17-20] has been used in the present work for prediction of residual stresses after spraying and subsequent heat treatments. The predicted effect of imposing a high through-thickness thermal gradient is shown in Fig.9. It can be seen that the stress level in the coating is moved towards more compressive values when the thermal gradient is imposed, particularly near the free surface. This is expected to accelerate the rates of sintering and stiffening, since it is now well-established [8] that these processes are retarded by the presence of tensile stresses – which hold open the microcracks and pores.

Conclusions

The following conclusions can be drawn from this work:

- The rate of sintering of plasma sprayed top coats in TBC systems is greater at higher temperatures and in the presence of more compressive in-plane residual stresses.
- The linear contractions associated with sintering are greater in the through-thickness direction than in the in-plane directions. This is a consequence of the splat and pore geometry in plasma sprayed top coats.
- The high thermal gradients commonly present in TBCs under service conditions lead to widely varying conditions within the top coat. Sintering is likely to occur much more rapidly near the free surface, not only because the temperatures are higher there, but because the residual stresses tend to be more compressive.

- Exposure to high temperatures near the free surface can also induce phase changes, which may affect the microstructure and the stress state. The as-sprayed top coat is entirely the non-transformable tetragonal T' phase. Isothermal heat treatment at 1300°C generated material with a substantial proportion of the cubic (F) phase. After heat treatment in a high thermal gradient, material near the bond coat remained entirely T' , whereas material near the free surface was composed of a mixture of low- and high-yttria tetragonal phases (T_1 and T_2), which were formed on cooling from the high temperature tetragonal (T) and cubic (F) phases respectively.

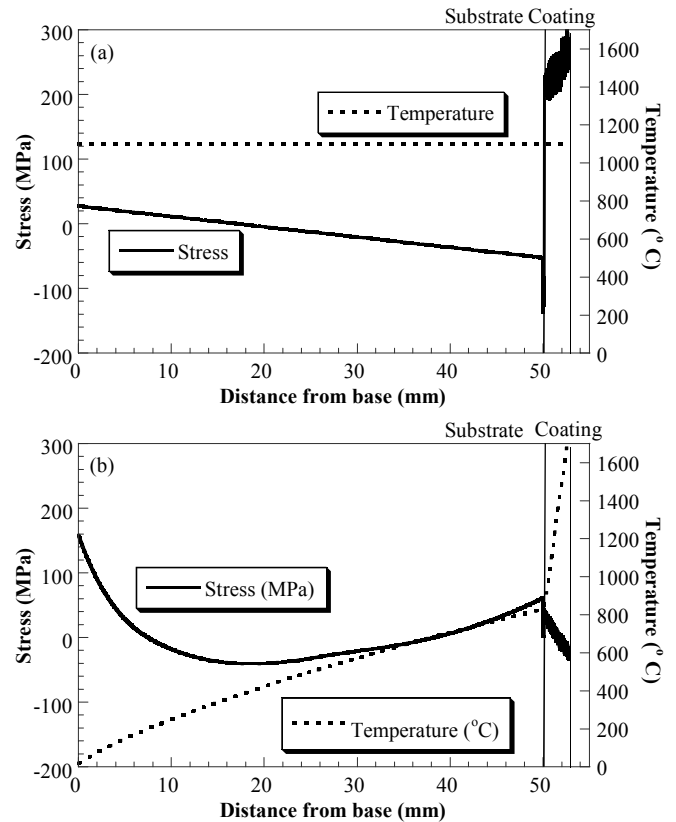


Figure 9: Predicted through-thickness distributions of stress and temperature in a TBC system (a) when isothermal at 1100°C and (b) when subjected to a high thermal gradient, similar to that employed in the experimental work.

Acknowledgements

This work is part of an ongoing program aimed at study of plasma sprayed thermal barrier coatings, supported by the EPSRC and by Rolls Royce and Sulzer Metco. One of the authors (SAT) has also received financial support from the Cambridge European Trust. There have been useful discussions with various industrial collaborators, particularly Dr. Rajiv Damani (Sulzer Innotec), Andrew Nicoll and Keith Harrison (Sulzer Metco).

References

1. M.P. Taylor, et al., "Observations of the Spallation Modes in an Overlay Coating and the Corresponding Thermal Barrier Coating System", *Mater. High Temp.*, 17 (2000) 219-224.
2. J. Rosler, M. Baker, and M. Volgmann, "Stress state and failure mechanisms of thermal barrier coatings: Role of creep in thermally grown oxide", *Acta Mater.*, 49 (2001) 3659-3670.
3. A.G. Evans, et al., "Mechanisms controlling the Durability of Thermal Barrier Coatings", *Prog. Mat. Sci.*, 46 (2001) 505-553.
4. R.A. Handoko, et al., "Mechanisms for Interfacial Toughness Loss in Thermal Barrier Coating Systems", *Key Eng. Mat.*, 197 (2001) 165-183.
5. T. Vogt, B.A. Hunter, and J. Thornton, "Structural evolution of thermal-sprayed yttria-stabilized ZrO₂ thermal barrier coatings with annealing - A neutron diffraction study", *J. Am. Ceram. Soc.*, 84 (2001) 678-680.
6. R. Vassen, G. Kerkhof, and D. Stover, "Development of a micromechanical life prediction model for plasma sprayed thermal barrier coatings", *Mater. Sci. Eng. A-Struct. Mater. Prop. Microstruct. Process.*, 303 (2001) 100-109.
7. J.W. Hutchinson and A.G. Evans, "On the delamination of thermal barrier coatings in a thermal gradient", *Surf. Coat. Technol.*, 149 (2002) 179-184.
8. J.A. Thompson and T.W. Clyne, "The Effect of Heat Treatment on the Stiffness of Zirconia Top Coats in Plasma-Sprayed TBCs", *Acta Mater.*, 49 (2001) 1565-1575.
9. T.W. Clyne, "Residual Stresses in Surface Coatings and their Effects on Interfacial Debonding", *Key Eng. Mat.*, 116/7 (1996) 307-330.
10. J.A. Thompson, J. Matejicek, and T.W. Clyne, "Modelling and Neutron Diffraction Measurement of Stresses in Sprayed TBCs", *Superalloys 2000*, T.M. Pollock, et al., TMS, Seven Springs, USA, 2000, 639-647.
11. H.E. Eaton and R.C. Novak, "Sintering Studies of Plasma Sprayed Zirconia", *Surf. Coat. Technol.*, 32 (1987) 227-236.
12. D.M. Zhu and R.A. Miller, "Sintering and Creep Behaviour of Plasma-Sprayed Zirconia- and Hafnia-Based Thermal Barrier Coatings", *Surf. and Coat. Techn.*, 109 (1998) 114-120.
13. I.R. Gibson, G.P. Dransfield, and J.T.S. Irvine, "Sinterability of Commercial 8 mol% Yttria-Stabilized Zirconia Powders and the Effect of Sintered Density on the Ionic Conductivity", *J. Mater. Sci.*, 33 (1998)
14. R. Vassen, et al., "Influence of Impurity Content and Porosity of Plasma-Sprayed Yttria-Stabilized Zirconia Layers on the Sintering Behaviour", *Surf. Coat. Technol.*, 141 (2001) 135-140.
15. J.A. Thompson and T.W. Clyne, "The Stiffness of Plasma Sprayed Zirconia Top Coats in TBCs", *United Thermal Spray Conference*, E. Lugscheider and P.A. Kammer, DVS, Dusseldorf, 1999, 835-840
16. H.G. Scott, "Phase Relationships in the ZrO₂-Y₂O₃ System", *J. Mat. Sci.*, 10 (1975) 1527-1535.
17. S.C. Gill and T.W. Clyne, "Stress Distributions and Material Response in Thermal Spraying of Metallic and Ceramic Deposits", *Met. Trans.*, 21B (1990) 377-385.
18. T.W. Clyne and S.C. Gills, "Heat Flow and Thermal Contraction during Plasma Spray Deposition", *Heat Flow and Thermal Contraction during Plasma Spray Deposition*, I. Tanasawa, Hemisphere, New York, 1991, 33-48
19. T.W. Clyne and S.C. Gill, "Residual Stresses in Thermally Sprayed Coatings and their Effect on Interfacial Adhesion - A Review of Recent Work", *J. Thermal Spray Technol.*, 5 (1996) 1-18.
20. Y.C. Tsui, J.A. Thompson, and T.W. Clyne, "The Effect of Bond Coat Creep on Residual Stresses and Debonding in Plasma Sprayed Thermal Barrier Systems", *Thermal Spray: Meeting the Challenges of the 21st Century. Proceedings of the 15th Int. Thermal Spray Conf.*, C. Coddet, ASM International, Nice, France, 1998, 1565-1570